Defining field output factors in small fields based on dose area product measurements: a feasibility study

Julien Jurczak, Benjamin Rapp, jean-marc bordy, Stéphanie Josset, Stephane Dufreneix

Defining field output factors in small fields based on dose area product measurements: a feasibility study

J. Jurczak[1,2], B. Rapp[1], J-M. Bordy[1], S. Josset[3], S. Dufreneix[1,3,*]

[1]CEA, List, Laboratoire National Henri Becquerel (LNE-LNHB), Palaiseau, France

[2]Institut Curie, Medical Physics Department, F-75005, Paris

[3]Institut de Cancérologie de l'Ouest, Angers/Saint-Herblain, France

*Corresponding author. E-mail: stephane.dufreneix@ico.unicancer.fr

Background: Dose area product in water (DAP_w) in small fields rely on the use of detectors with a sensitive area larger than the irradiation field. This quantity has recently been used to establish primary standards down to 5 mm field size with an uncertainty smaller than 0.7%. It has the potential to decrease the uncertainty related to field output factors but it is not currently integrated into treatment planning systems.

Purpose: The aim of this study was to explore the feasibility of converting a DAP_w into a point dose in small fields through the determination of a volume averaging correction factor. By determining the field output factors, a comparison between the so-called "DAP_w to point dose" approach and the IAEA TRS483 methodology was performed.

Method: Diodes, diamonds and a micro ionization chamber were used to measure field output factors following the IAEA TRS483 methodology on two similar linacs equipped with circular cones down to 6 mm diameter. For the "DAP_w to point dose" approach, measurements were performed with a dedicated and built-in-house 3 cm diameter plane-parallel ionization chamber calibrated in terms of DAP_w in the French Primary Dosimetry Standards Laboratory LNE-LNHB. Beam profile measurements were performed to generate volume averaging correction factors enabling the conversion of an integral DAP_w measurement into a point dose and the determination of the field output factors. Both sets of field output factors were then compared.

Results: By following the IAEA TRS483 methodology, field output factors agreed within ±3% for all detectors on both linacs. Large variation were observed for the volume averaging correction factors with a maximum spread between the detectors of 26% for the smallest field size. Consequently, deviations up to 15% between the "IAEA TRS483" and the "DAP_w to point dose" methodologies were found for the field output factor of the smallest field size. It was attributed to the difficulty of accurately determine beam profiles in small fields.

Conclusion: Although primary standards associated to small uncertainties can be established in terms of DAP_w in a primary laboratory, the "DAP_w to point dose" methodology requires a volume averaging correction to derive a field output factor from DAP_w measurements. None of the point detector studied provided satisfactory results and additional work using other detectors such as film is still required to allow the transfer of a DAP primary standard to users in terms of absorbed point dose.

Keywords: *small field, output factor, dose area product*

1. Introduction

Small field measurements remain challenging due to the loss of lateral charged particle equilibrium, the occlusion of the primary photon source and the size of the detector relative to the size of the radiation field which generates volume averaging over the detector sensitive area and perturbation of the particle fluences [1,2]. In a primary dosimetry standards laboratory, calorimetric measurements could be performed in terms of absorbed dose at a point in water for field sizes down to 2 cm x 2 cm [3,4]. In radiation oncology departments, small field output factors are measured with dedicated detectors following the IAEA TRS483 code of practice [1].

An alternative approach to point dose measurements in small fields was proposed by performing integral measurements with detectors larger than the irradiation field [5–7]. A new metric, the dose area product in water (DAP_w) was introduced. It represents the energy per mass deposited by the beam over the sensitive area of the detector and is expressed in $Gy.cm^2$. It can be interpreted as the integral of the absorbed dose distribution over the sensitive area of the detector. As a consequence, the absorbed dose D_{abs} at a point located at (x,y) distance from the axis has a contribution to the dose integral depending on (x,y) distances. An example in a circular field and assuming a cylindrical geometry is given in Figure 1: the most important contribution to the DAP comes from the penumbra region of the beam profile and profile tails have a contribution that cannot be neglected. DAP_w properties were investigated [8–10] and primary standards were established in terms of DAP_w for field sizes ranging from 5 mm to 15 mm [11,12] using a new designed large section graphite calorimeter. Dedicated and built-in-house large section plane-parallel ionization chambers were then calibrated, with a relative standard uncertainty smaller than 0.7 % for all calibration coefficients in small fields [12].

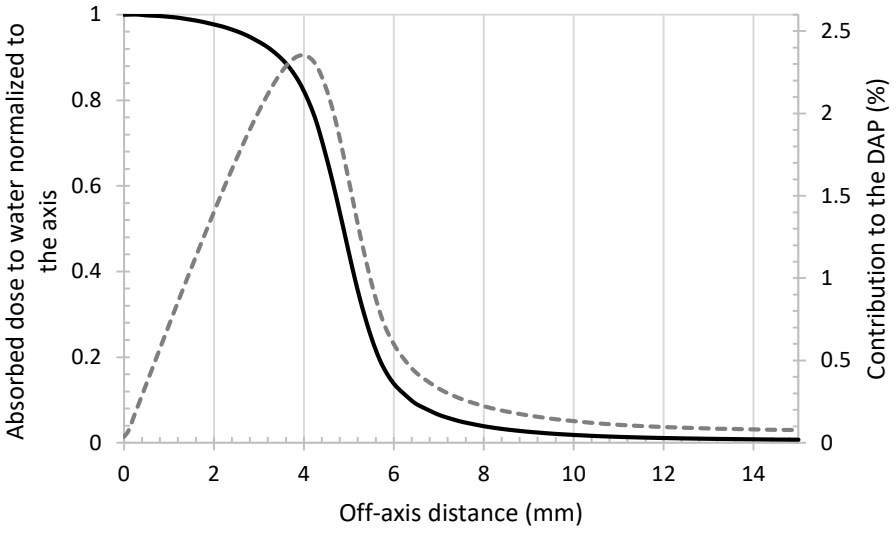

Figure 1 : Example of the variation of absorbed dose to water with off-axis distance (solid line, left axis) and its corresponding contribution to the dose integral (dotted line, right axis) in a 10 mm diameter field.

The clinical implementation of the DAP_w based on measurements with a large section plane-parallel ionization chamber has however not yet been investigated. The most direct option to exploit DAP primary standards would be to introduce DAP_w in treatment planning systems (TPS). This would require a formalism modification in TPS at least the for output factor input data, considering an integrated measurement instead of a point dose. Another and easier solution would be to convert DAP_w measurements into point dose thanks to a volume averaging correction factor ideally generated from a 2D dose mapping of the beam. A 1.2% difference was previously observed between a calibration coefficient derived from DAP_w measurements and one directly established in terms of absorbed dose to water at a point in a square 2 cm field [13]. However, no other studies investigated the link between DAP_w and point dose for smaller field sizes and the transfer of primary standards measurements to radiation oncology departments is still to be formalized.

The aim of this study was to explore the feasibility of using the DAP_w quantity in a radiation oncology department for small fields through a conversion into point dose. Measurements were performed in circular field sizes down to 6 mm diameter using a large section plane-parallel ionization chamber calibrated in terms of DAP_w at the French Primary Dosimetry Standards Laboratory LNE-LNHB. Several solid point detectors were used to define the field output factors following the IAEA TRS483 methodology [1]. Assuming an axial symmetry, the volume averaging factors were determined based on profile measurements with the different point detectors. Field output factors derived from the large section plane-parallel ionization chamber measurements and combined with the volume averaging correction factors were compared to field output factors derived from the IAEA TRS483 methodology [1].

2. Materials and methods

2.1. Plane-parallel ionization chamber and formalism

The large section plane-parallel ionization chamber, denoted reference chamber afterwards was designed and built in-house at the French primary dosimetry standards laboratory LNE-LNHB [12]. Developed for measurements in small fields up to 15 mm, its collection area has a diameter of 30 mm enabling the integration of the energy deposited by the beam over its sensitive area.

For the purpose of this study, the reference ionization chamber was calibrated in terms of absorbed dose to water D_w ($Gy.C^{-1}$) in a 10 cm x 10 cm field in a 6 MV FFF beam at the laboratory, using water calorimetry as a primary standard, according to the expression:

$$N_{D,w,fref} = \left[\frac{D_w}{Q_w^*}\right]_{fref} \quad (1)$$

Where:

- $N_{D,w,fref}$ (in $Gy.C^{-1}$) is the calibration coefficient in terms of absorbed dose to water at a point
- D_w is the absorbed dose to water at a point measured by water calorimetry
- Q_w^* is the collected charge measured by the reference ionization chamber and corrected from the influence quantities (temperature, pressure, polarity, recombination and volume averaging over its collection area)

This reference chamber was also calibrated in terms of dose area product in water DAPw ($Gy.cm^2.C^{-1}$) in a 6 MV FFF beam for various circular field sizes (denoted f_{clin}) ranging from 5 to 15 mm diameter, using graphite calorimetry as a primary standard, according to the expression:

$$N_{DAP,w,f_{clin}} = \left[\frac{DAP_w}{Q_w^*}\right]_{f_{clin}} = \left[\frac{D_{core}}{Q_w^*}\right]_{f_{clin}} \left[\frac{D_w}{D_{core}}\right]_{MC,f_{clin}} S_{core} k_i \quad (2)$$

Where:

- $N_{DAP,w}$ (in $Gy.cm^2.C^{-1}$) is the calibration coefficient in terms of DAP_w
- DAP_w is the dose-area product in water
- D_{core} is the average absorbed dose in the core (sensitive part) of the calorimeter
- $\left[\frac{D_w}{D_{core}}\right]_{MC}$ is the graphite to water dose conversion factor calculated by Monte Carlo
- S_{core} is the core area
- k_i an impurity correction factor taking into account the effects on the absorbed dose of all the impurities within the core that are different from graphite (mainly thermistors for temperature measurement). This correction was considered here dosimetrically negligible because thermistors are located at the periphery of the core and are not in the direct beam.

Details on the reference chamber and its calibration coefficients can be found in [12]. Since $N_{DAP,w,f_{clin}}$ was found slightly dependent on field size, calibration coefficients in terms of DAP_w were defined for each field size studied by linearly interpolating to the corresponding measured FWHM.

Derived from equation (2), the absorbed dose to water at a point located on the beam axis, in a clinical field, can be expressed as:

$$D_{w,f_{clin}} = \frac{N_{DAP,w,f_{clin}} Q^*_{w,f_{clin}}}{S_{core} k_i} \quad (3)$$

A field output factor $\Omega_{Q_{clin},Q_{ref}}^{f_{clin},f_{ref}}$ measured by the reference chamber can then be defined as:

$$\Omega_{Q_{clin},Q_{ref}}^{f_{clin},f_{ref}} = \frac{D_{w,f_{clin}}}{D_{w,f_{ref}}} = \frac{1}{S_{core}k_i}\frac{N_{DAP,w,f_{clin}}}{N_{D,w,fref}}\frac{Q^*_{w,f_{clin}}}{Q^*_{w,f_{ref}}} \quad (4)$$

The numerator of the formula for f_{clin} is based on the DAP_w formalism whereas the denominator of the formula for f_{ref} is based on the usual point dose formalism. $N_{DAP,w,f_{clin}}$, $N_{D,w,f_{ref}}$, S_{core} and k_i were provided by the primary standards laboratory. $Q^*_{w,f_{clin}}$ and $Q^*_{w,f_{ref}}$ were measured with the reference chamber in two radiation oncology departments. Those last quantities are the collected charge corrected from influence quantities: temperature, pressure, polarity, recombination and volume averaging over its collection area. Details and formulas for the correction factors for the influence quantities can be found in the IAEA TRS398 [14] and IAEA TRS483 [1]. Of specific interest for this study is the volume averaging correction factor. It can be expressed as [1,15]:

$$k_{vol} = \frac{\iint_A dxdy}{\iint_A OAR(x,y)dxdy} \quad (5)$$

Where:

- x and y are the coordinates on the axes orthogonal to the beam central axis
- A is the area of the projection of the sensitive volume of the reference chamber on a plane orthogonal to the beam axis
- OAR(x,y) is the off-axis ratio, which is the 2-D lateral beam profile at the measurement depth normalized to unity on the central axis

In a 10 cm x 10 cm reference field, the volume averaging correction factor is close to unity, even for a large sensitive area in a FFF beam: for example, $k_{vol,f_{ref}}$=1.0067 for the 30 mm diameter sensitive area of the reference chamber in a 6 FFF beam. However, for fields f_{clin} smaller than the sensitive area of the reference chamber, it strongly increases with decreasing field size since the sensitive area is no longer homogeneously irradiated. Measurement of the off-axis ratio OAR(x,y) in the radiotherapy departments for the small fields studied is then needed. Ideally, the determination of $k_{vol,f_{clin}}$ requires a complete 2D mapping of the beam over the sensitive area and radiochromic films seem to be good candidates considering their water equivalency and high spatial resolution. However, they are associated to a potential penumbra blurring that need to be taken into account [2]. Their use also remain challenging to perform accurate dose measurements [16]. Point detectors can also be used by assuming the axial symmetry of the circular cones. Only a hemi-profile could be used to determine $k_{vol,f_{clin}}$ following the equation:

$$k_{vol} \approx \frac{\int_0^{R_A} rdr}{\int_0^{R_A} OAR(r)dr} \quad (6)$$

Where R_A is the radius of the sensitive area of the reference chamber.

2.2. Detectors and setup

Measurements were performed on two Varian TrueBeam STx (Varian Medical Systems, Palo Alto, CA, USA) named Linac1 and Linac2 in a 6 MV FFF beam (1400 MU/min), at 10 cm depth in water and 90 cm SSD. Field sizes were defined by circular cones of 15, 12.5, 10, 7.5 and 6 mm nominal diameter manufactured by Brainlab (Brainlab AG, Munich, Germany) while the jaws were set to a 20 mm x 20 mm square field. Each Linac had its own set of cones.

Five consecutive charge measurements, each over 20 s, were performed with the reference chamber for each circular cone, in a single measurement session. A 10 cm x 10 cm reference field was measured before and after each cone measurement to correct from a potential drift of the accelerator.

Detectors used in this study for field output factor and $k_{vol,f_{clin}}$ determination are summarized in Table 1. All solid dosimeters were positioned with their axis parallel to the beam axis. Reference chamber measurements were performed perpendicular to the beam. The IBA_Razor_Nanochamber axis was positioned parallel to the beam for the profile measurement to avoid any stem effect while it was positioned perpendicular to the beam for the field output factor determination to minimize the k_{pol} and k_{rec} corrections [17]. Some models (PTW_60018 and PTW_60019) were doubled to evaluate the intra-model reproducibility.

Table 1 : Detectors used in this study

Name	Linac1	Linac2	Type	Active material / additional components	Diameter of the sensitive area (mm)	Typical sensitivity (nC/Gy)
Reference chamber	x	x	Ionization chamber	Air cavity Electrodes: graphite Wall: cross-linked polystyrene	30	NA (depending on field size)
IBA_Razor Nanochamber	x		Ionization chamber	Air cavity Central electrode: Graphite Wall: Shonka (C-552)	2	0.11
IBA_SFD	x	x	Stereotactic field diode	Silicon Wall: ABS + Epoxy resin	0.6	6
PTW_60017	x	x	Diode E	Silicon Wall: RW3 + Epoxy resin	0.6	9
PTW_60018_1 *(SN 000186)*	x	x	Diode SRS	Silicon Wall: RW3 + Epoxy resin	0.6	175
PTW_60018_2 *(SN 000434)*	x					

PTW_60019_1 *(SN 122271)*	x	x	Diamond	Carbon Wall: RW3 + Epoxy resin	2.2	1
PTW_60019_2 *(SN 123788)*	x					

174

175 *2.3. Field output factors*

176 Field output factors were determined for point detectors listed in Table 1. For each detector, a pre-
177 irradiation of at least 1000 MU was performed before acquiring two profiles in the crossline and inline
178 directions for centering with the smallest 6 mm diameter cone. A 10 cm x 10 cm reference field was
179 measured before and after each cone measurement. Each time a cone was set up, two profiles were
180 performed to verify (and correct if necessary) the alignment of the detector on central axis before
181 performing the point dose measurement. On the beam axis, an average over 3 charge readings was
182 considered.

183 The $k_{Q_{clin},Q_{msr}}^{f_{clin},f_{msr}}$ correction factors defined in the IAEA TRS-483 [1] were applied for the diodes and
184 diamond detectors. Since the IBA Razor Nanochamber was not listed in the IAEA TRS-483, no
185 correction factor was applied. For this detector, Partanen *et al.* reported a 1.034 correction factor in a
186 5 mm field at 6 MV FFF [18] but Lopez-Sanchez *et al.* reported a 1.005 correction factor for similar
187 conditions [19].

188 The field output factor derived from the reference chamber measurements was compared to the
189 average field output factor over all point detectors. Data were reported respective to the equivalent
190 square field size defined as:

191 $$S_{clin} = r\sqrt{\pi}$$

192 Where r is the circular field radius defined by the points where, on average, the dose level amounts to
193 50% of the maximum dose at the measurement depth [1]. Profiles measured with the PTW_60018_1
194 detector were arbitrarily taken for the determination of r but all detectors gave r values within 0.1 mm.

195

196 *2.4. Determination of $k_{vol,f_{clin}}$*

197 Profiles measured by point detectors listed in Table 1 were used, with a 0.1 mm resolution between
198 -15mm and +15mm in the crossline and inline directions. Minimum acquisition time was 1s per step
199 and beam profiles were normalized on the axis. For each cone, the mean $k_{vol,f_{clin}}$ over the 4 hemi-
200 profiles was considered and the standard deviation was reported.

201 A $k_{vol,f_{clin}}$ value was thus determined for each cone and each detector (i.e. 40 k_{prof} values).
202 Following equation (4), a field output factor was derived and compared to the average field output factor
203 over all point detectors defined in section 2.3.

204

205 **3. Results**

206 *3.1. Field output factors*

Deviation of individual field output factors per detector compared to the mean value over all detectors is visible in Figure 2 for the different S_{clin} studied. The correspondence between field size and S_{clin} is provided in Table 2. All measurements agree with ± 3%, even for the uncorrected values of the IBA Razor Nanochamber. A good reproducibility is observed between two detectors of the same type (PTW 60018 and PTW 60019) with a maximum deviation of 0.4%. A good reproducibility is also observed between the two linacs: except for the measurement with the IBA SFD in the smallest circular field (2.2%), the maximum deviation is 0.5%.

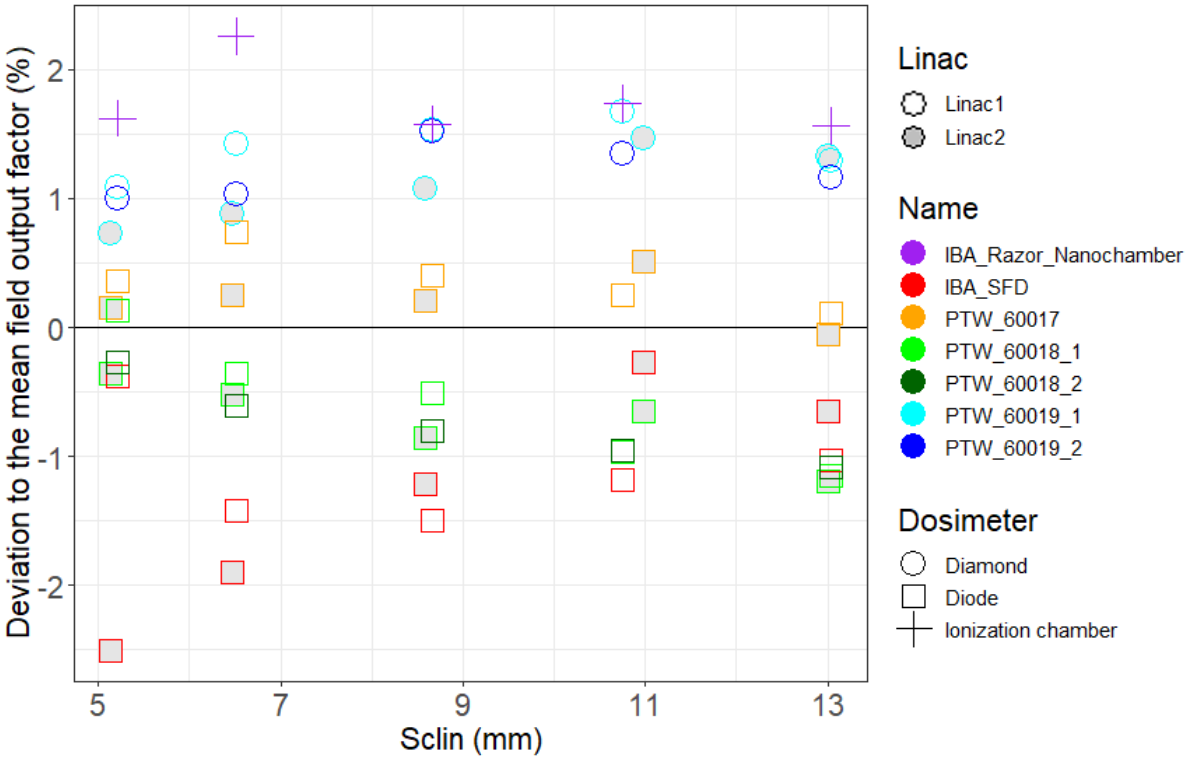

Figure 2 : deviation of field output factors compared to the mean value over all detectors.

The average field output factors taken as a reference for the comparison of the DAP_w and point dose approaches are given in Table 2. The mean relative standard deviation associated is 1.2%. A comparison with Monte Carlo field output factors calculated by Hermida-Lopez *et al.* [20] shows a maximum deviation of 3.2% which is similar to the deviations observed by these authors in their literature review. These authors also provided an experimental field output factor for a 7.5 mm diameter cone based on measurements with PTW_60019 SFD and EBT3 films. They found a value of 0.65 in agreement with our study (0.4% deviation).

Table 2 : mean field output factor and their associated standard deviation.

Field size (mm)	S_{clin} (mm)	Mean $\Omega_{Q_{clin},Q_{ref}}^{f_{clin},f_{ref}}$ (1 SD)	Hermida-Lopez *et al.* [20]	
			MC value	Deviation (ref: [20])
15	13.0	0.760 (0.009)	0.78	-2.6%
12.5	10.9	0.736 (0.008)	0.76	-3.1%
10	8.6	0.701 (0.008)	0.72	-2.6%

7.5	6.5	0.653 (0.008)	0.67	-2.6%
6	5.2	0.608 (0.007)	0.62	-1.9%

3.2. $k_{vol,f_{clin}}$ values

An example of measured relative profile in the 6 mm circular cone is shown in Figure 3. As expected, differences are observed in the penumbra region: the IBA_Razor_Nanochamber gives the smoothest penumbra whereas the IBA_SFD gives the sharpest. An overall good reproducibility between the 2 PTW_60018 is observed. The 2 PTW_60019 detectors are in agreement in the penumbra region but slightly differ in the profile tails: at 15 mm from the axis, the dose measured by the PTW_60019_2 (0.5%) is approximatively twice the one measured by the PTW_60019_1 (0.2%). Fluctuations of 0.05% are observed for the IBA_Razor_Nanochamber in the profile tails probably linked to the small sensitive volume of the ionization chamber and its associated poor sensitivity (Table 1). The integration time was not increased to reduce the noise for this detector in order to keep the overall measurement session duration reasonable (approximatively 2 hours for the 5 small profiles, without considering the output factor measurements).

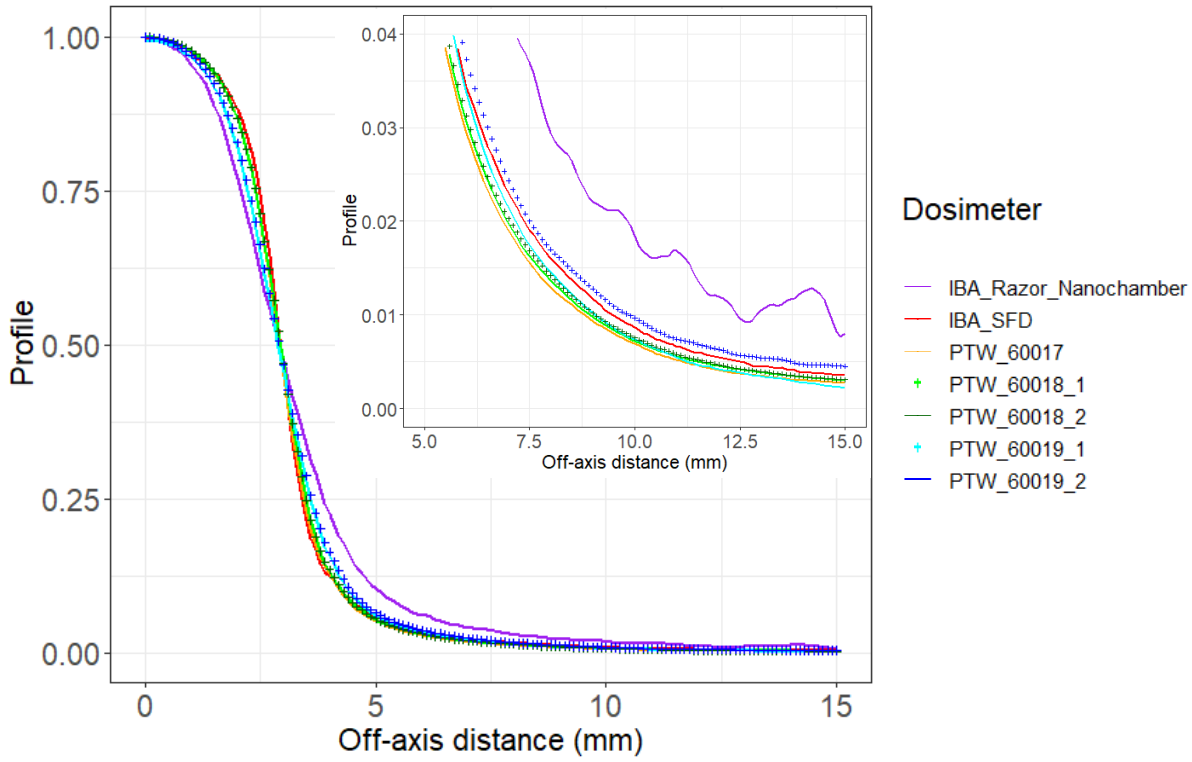

Figure 3 : Hemi beam profiles normalized on the axis measured with various point detectors in the 6 mm circular cone on Linac1.

For each detector and field size, the mean $k_{vol,f_{clin}}$ values calculated from the relative profiles are reported in Table 3 with their associated standard deviations $k_{vol,f_{clin}}$ values increases when the field size decreases enlightening the importance of the contribution of profile penumbra and tail to the dose

integral. Standard deviations range between 0.1% and 2.7% and generally increase when the field size decreases. These values confirmed the hypothesis that an axial geometry can be assumed.

A large variability of the $k_{vol,f_{clin}}$ is observed depending on the detector considered: for a specific linac and field size, the spread of $k_{vol,f_{clin}}$ values increases from 4.4% for the 15 mm circular cone to 25.8% for the 6 mm circular cone. $k_{vol,f_{clin}}$ values for the IBA_Razor_Nanochamber are noticeably smaller than the values derived from solid detectors. Some profiles measured with the same detector on both linacs either give relatively close $k_{vol,f_{clin}}$ values (PTW_60017 and PTW_60018_1), or give differences up to 17% (IBA_SFD and PTW_60019_1). Profile measurements on Linac1 with the PTW_60018_1 and PTW_60018_2 give $k_{vol,f_{clin}}$ values in agreement within 1% whereas differences up to 13% are observed between PTW_60019_1 and PTW_60019_2.

Table 3 : $k_{vol,f_{clin}}$ values derived from profiles or 2D dose map measurements for several detectors. Standard deviations are given in parenthesis.

		Cone diameter / S_{clin} (mm)				
Detector	Linac	15 / 13.0	12.5 / 10.9	10 / 8.6	7.5 / 6.5	6 / 5.2
IBA_SFD	Linac1	3.84 (0.05)	5.43 (0.04)	8.02 (0.08)	13.1 (0.1)	18.9 (0.2)
	Linac2	3.85 (0.01)	5.20 (0.01)	8.08 (0.08)	13.1 (0.2)	18.9 (0.2)
	Deviation Linac2/Linac1	*0.3%*	*-4.2%*	*-0.8%*	*-0.3%*	*-0.1%*
PTW_60017	Linac1	3.87 (0.01)	5.48 (0.04)	8.17 (0.04)	13.4 (0.2)	19.8 (0.4)
	Linac2	3.91 (0.01)	5.33 (0.02)	8.33 (0.03)	13.6 (0.2)	20.0 (0.2)
	Deviation Linac2/Linac1	*1.2%*	*-2.8%*	*2.0%*	*2.2%*	*1.4%*
PTW_60018_1	Linac1	3.85 (0.01)	5.46 (0.02)	8.07 (0.04)	13.3 (0.1)	19.3 (0.2)
	Linac2	3.85 (0.01)	5.23 (0.04)	8.16 (0.04)	13.3 (0.2)	19.6 (0.2)
	Deviation Linac2/Linac1	*0.0%*	*-4.2%*	*1.2%*	*0.2%*	*1.3%*
PTW_60018_2	Linac1	3.83 (0.02)	5.46 (0.04)	8.07 (0.05)	13.2 (0.1)	19.2 (0.0)
Deviation PTW_60018_1/ PTW_60018_2		*0.7%*	*0.1%*	*-0.1%*	*0.4%*	*0.8%*
PTW_60019_1	Linac1	3.90 (0.06)	5.53 (0.04)	8.17 (0.10)	13.4 (0.1)	19.3 (0.1)
	Linac2	3.78 (0.02)	5.08 (0.02)	7.83 (0.06)	12.3 (0.2)	17.2 (0.3)
	Deviation Linac2/Linac1	*-3.1%*	*-8.1%*	*-4.1%*	*-8.6%*	*-10.7%*
PTW_60019_2	Linac1	3.83 (0.01)	5.40 (0.02)	7.95 (0.07)	12.9 (0.2)	18.3 (0.1)
Deviation PTW_60019_1/ PTW_60019_2		*-0.6%*	*-0.9%*	*5.9%*	*9.1%*	*12.6%*
IBA_Razor_Nanochamber	Linac1	3.74 (0.01)	5.27 (0.05)	7.49 (0.15)	11.5 (0.2)	15.2 (0.4)

3.3. Comparison of the DAP_w and point dose approaches

Figure 4 shows the DAP_w measured with the reference chamber on the two linacs. Errors bars are plotted considering a 0.63% uncertainty on the $N_{DAP,w,f_{clin}}$ [12] and a repeatability of 0.05% but they are

smaller than the symbols. This confirms that DAP measurements associated to a small uncertainty can be performed in radiation oncology departments in small fields.

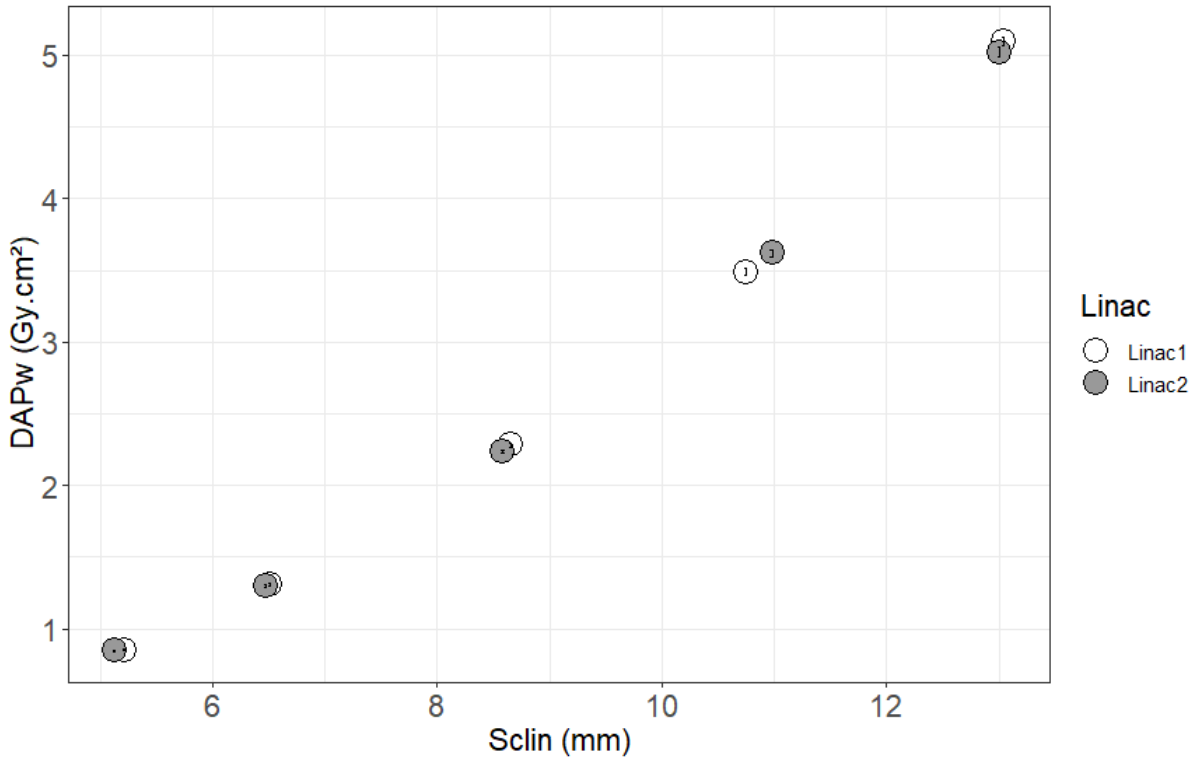

Figure 4 : DAP_w measured by the reference chamber on two linacs

Using $k_{vol,f_{clin}}$ values, field output factors were derived from the DAP_w measurement with the reference chamber associated to profiles measurements for each detectors. The comparison against the mean field output factors defined in section 3.1. is shown in Figure 5. Large deviations (up to 14% for the smallest field size) are observed and no detector used for the determination of the $k_{vol,f_{clin}}$ value gives a field output factor in agreement with the reference within 5 % for all field sizes. For the two largest fields (15 and 12.5 mm diameter), a mean deviation of 4% is found between the "DAP to dose point" and the IAEA TRS 483 methodologies. Deviation then increases with decreasing field size with a quasi-systematic overestimation of the value derived from DAP_w measurements for solid detectors whereas a large underestimation is observed for the IBA_Razor_Nanochamber. Results for the PTW_60019 show a large variability between the 2 linacs and between PTW_60019_1 and PTW_60019_2. This is attributed to the variability of the measurements in the profile tails: for the 6 mm field size, at 15 mm from the axis, the relative dose measured by the PTW_60019_1 is 0.2% on Linac1 and 0.8% on Linac2 whereas the dose measured with the PTW_60019_2 is 0.5% on Linac1. On the contrary, the profile penumbra and tail measured by the IBA_SFD and PTW_60018 are much more reproducible: 0.4% for the IBA_SFD at 15 mm from the axis on both linacs and 0.3% for the PTW_60018_1 on both linacs and PTW_60018_2. These small differences have a non-negligible impact on the volume averaging correction factor since the integration is performed on a 15 mm radius circle.

The surface covered by the profile penumbra and tail is thus important as their contribution to the dose integral.

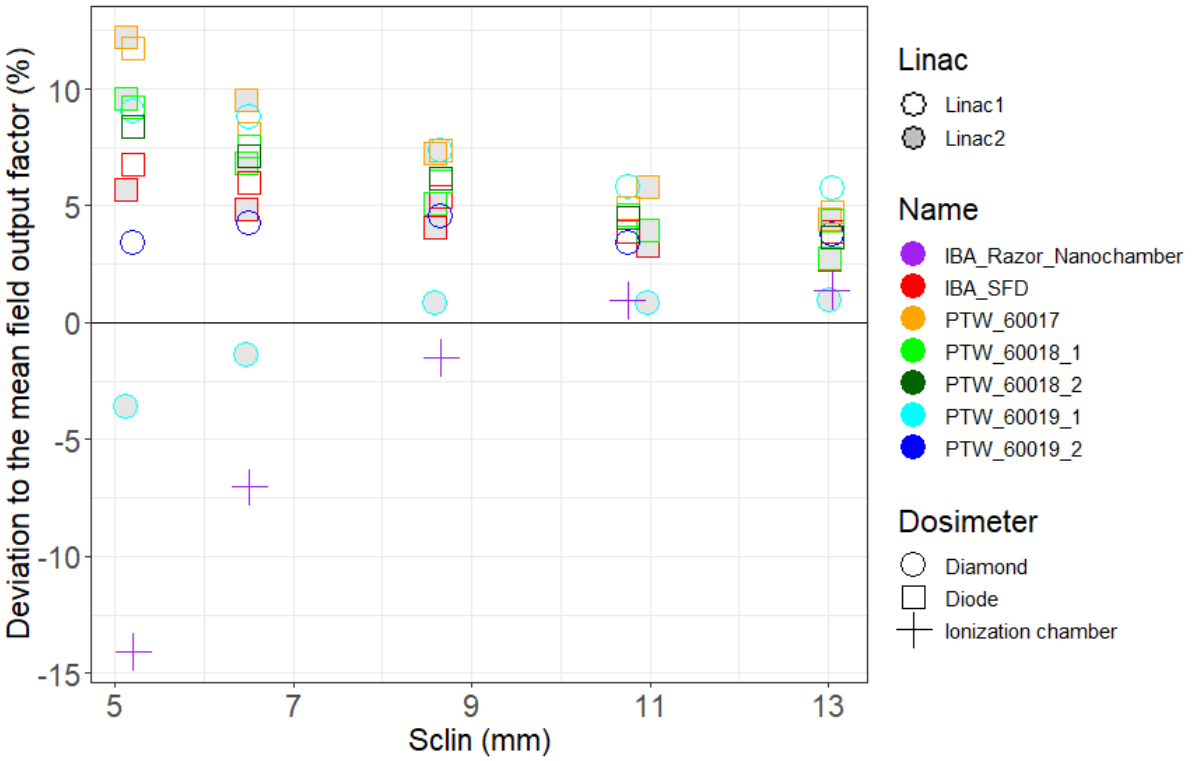

Figure 5 : Field output factors derived from a DAP_w measurement and a $k_{vol,f_{clin}}$ value for various detectors. Deviation against the mean field output factor defined in 3.1. is plotted.

4. Discussion

This study evaluated the feasibility of deriving a field output factor in small fields from measurements with a reference chamber calibrated in terms of DAP_w. The formalism to do so requires a volume averaging correction factor to determine the dose integral over the sensitive area of the reference chamber. Results show that this correction factor is critical and that none of the detectors studied provide a satisfactory "DAP_w to point dose" conversion based on such profile measurements. A large spread of the $k_{vol,f_{clin}}$ values is observed stressing that the commercial detectors studied could not be used for the "DAP_w to point dose methodology". The intra-model reproducibility for the PTW_60018 and PTW_60019 shows contrasted results: a relative good agreement is observed for the PTW_60018 (4.2 % maximal dispersion on the $k_{vol,f_{clin}}$ values for both detectors and linacs) but a maximum 12.6 % dispersion is observed for the PTW_60019. This adds a difficulty to transfer DAP_w primary standards to radiation oncology departments in terms of point dose since the conversion should not depend on the specific detector used for the profile measurement. Although robust for the establishment of primary standards in small fields, the DAP_w approach suffer difficulties to be transfered to users in terms of point dose. The variation between detectors for field output factor measurements (±3%) in the IAEA TRS483 approach is replaced and magnified in the DAP_w approach by the variation between detectors for beam

302 profile measurements. This study highlights the difficulty to accurately determine a beam profile in
303 small fields and especially the scatter dose far from the axis where the energy dependence of the
304 detectors is of primary importance [21]. The ideal detector for profile measurements in small fields should
305 have a small sensitive volume to avoid incorrect determination of the width of the penumbra and be the
306 least perturbing tissue equivalent [2]. Francescon *et al.* calculated with Monte Carlo correction factors for
307 profile measurements as a function of off-axis distance [22]. Large correction factors (up to 1.3) were
308 reported after the geometric field edge depending on the detector. The PTW_60019 showed the smallest
309 correction factors but still underestimated the dose up to 5 % at 8 mm from the central axis (for a
310 geometric field edge at 4 mm). Lopez-Sanchez et al. also reported correction factors between 0.8 and
311 1.1 in the penumbra region of a 5 mm circular cone for two ionization chambers including the
312 IBA_Razor_Nanochamber [19]. Similarly, Underwood et al. reported large variation of the correction
313 factor with off-axis distance for a PTW_60003 Diamond detector and a PTW_31006 PinPoint ionization
314 chamber [23]. No current commercially available point detector seems to be adequate for profile
315 measurements in small fields.
316 One default of the formalism applied to the solid detectors used in this study is that the beam profile
317 is normalized to the beam axis without considering the fact that each detector has its own and different
318 response on the beam axis for a given field size. However, as observed by Underwood *et al.* [23], the
319 under- or over-response of a detector on the beam axis could be compensated by an over- or under-
320 response on the tails by normalizing the beam profiles to the detector's response in a 10 cm x 10 cm
321 beam. At the end, such calibrated beam profiles could lead to a unique dose area product without any
322 detector effect. Here, by normalizing the beam profile on the axis, the under- or over-response on the
323 beam axis is ignored and there cannot be a compensation between the beam axis and the tails. The over-
324 response at the tails can be even amplified or the under-response reduced, thus affecting the k_{vol}
325 calculation. However, the calibrated beam profiles described by Underwood *et al.* [23] are not compatible
326 with the formalism proposed here : a normalized profile is needed to calculate the dose on the beam axis
327 and consequently the detector used to measure the beam profile needs to be energy-independent on the
328 beam axis and off axis. Solid detectors remain useful to check the consistency of the k_{vol} calculation.
329 Future work will include the investigation of radiochromic films and the development of an in-house
330 film optical reader compatible with metrological applications. The 2D dose mapping of the beam could
331 then be measured and the cylindrical symmetry of the circular cones would not be needed. k_{vol} could
332 then be determined using equation (5). Other tissue equivalent point detectors like plastic scintillator
333 could also be evaluated.
334

335 **5. Conclusion**

336 Two methodologies were compared to determine field output factor in small fields: the first
337 described in the IAEA TRS483 based on point dose measurements and the second based on dose area
338 product measurements with a large reference chamber, associated to volume averaging correction

derived from profiles or 2D dose map measurements. Reference field output factors based on point measurements were determined on two linacs with several detectors. A standard deviation over all detector smaller than 1.4% was achieved. Volume averaging correction factors were determined with numerous detectors and showed large variations depending on the detector with a spread up to 26% for the smallest field size. Due to this large variability depending on the detector used for the profile measurement, the DAP_w to point dose methodology can not easily be transferred to users in terms of absorbed dose at a point although it is promising to establish dosimetric standards in a primary laboratory.

References:

1. IAEA, AAPM. *Dosimetry of Small Fields Used in External Beam Radiotherapy*. International Atomic Energy Agency Technical Report Series 483; 2017.

2. Das IJ, Francescon P, Moran JM, et al. Report of AAPM Task Group 155: Megavoltage photon beam dosimetry in small fields and non-equilibrium conditions. *Med Phys*. 2021;48(10):e886-e921. doi:10.1002/mp.15030

3. Krauss A, Kapsch RP. Experimental determination of kQ factors for cylindrical ionization chambers in 10 cm × 10 cm and 3 cm × 3 cm photon beams from 4 MV to 25 MV. *Phys Med Biol*. 2014;59(15):4227-4246. doi:10.1088/0031-9155/59/15/4227

4. Delaunay F, Kapsch RP, Gouriou J, et al. Comparison of absorbed-dose-to-water units for Co-60 and high-energy x-rays between PTB and LNE–LNHB. *Metrologia*. 2012;49:S203-S206.

5. Djouguela A, Harder D, Kollhoff R, Rühmann A, Willborn KC, Poppe B. The dose-area product, a new parameter for the dosimetry of narrow photon beams. *Z Med Phys*. 2006;16(3):217-227. doi:10.1078/0939-3889-00317

6. Sánchez-Doblado F, Hartmann GH, Pena J, Roselló JV, Russiello G, Gonzalez-Castaño DM. A new method for output factor determination in MLC shaped narrow beams. *Phys Med*. 2007;23(2):58-66. doi:10.1016/j.ejmp.2007.03.002

7. Niemelä J, Partanen M, Ojala J, et al. Measurement and properties of the dose-area product ratio in external small-beam radiotherapy. *Phys Med Biol*. 2017;62(12):4870-4883. doi:10.1088/1361-6560/aa6861

8. Niemela J, Partanen M, Ojala J, et al. Measurement and properties of the dose-area product ratio in external small-beam radiotherapy. *Phys Med Biol*. 2017;62(12):4870-4883. doi:10.1088/1361-6560/aa6861

9. Niemelä J, Partanen M, Ojala J, Kapanen M, Keyriläinen J. Dose-area product ratio in external small-beam radiotherapy: beam shape, size and energy dependencies in clinical photon beams. *Biomed Phys Eng Express*. 2021;7(3). doi:10.1088/2057-1976/abf6aa

10. Pimpinella M, Caporali C, Guerra AS, et al. Feasibility of using a dose-area product ratio as beam quality specifier for photon beams with small field sizes. *Phys Med*. 2018;45:106-116. doi:10.1016/j.ejmp.2017.12.012

11. Dufreneix S, Ostrowsky A, Le Roy M, et al. Using a dose-area product for absolute measurements in small fields: a feasibility study. *Phys Med Biol*. 2016;61(2):650-662. doi:10.1088/0031-9155/61/2/650

12. Jurczak J, Rapp B, Delaunay F, Gouriou J, Dufreneix S, Bordy JM. Dose area product primary standards established by graphite calorimetry at the LNE-LNHB for small radiation fields in radiotherapy. *Phys Med*. 2022;98:18-27. doi:10.1016/j.ejmp.2022.03.013

13. Dufreneix S, Ostrowsky A, Rapp B, Daures J, Bordy JM. Accuracy of a dose-area product compared to an absorbed dose to water at a point in a 2 cm diameter field. *Med Phys*. 2016;43(7):4085. doi:10.1118/1.4953207

14. IAEA. Absorbed Dose Determination in External Beam Radiotherapy: An International Code of Practice for Dosimetry based on Standards of Absorbed Dose to Water. Published online 2006.

15. Kawachi T, Saitoh H, Inoue M, Katayose T, Myojoyama A, Hatano K. Reference dosimetry condition and beam quality correction factor for CyberKnife beam. *Med Phys*. 2008;35(10):4591-4598. doi:10.1118/1.2978228

16. Niroomand-Rad A, Chiu-Tsao ST, Grams MP, et al. Report of AAPM Task Group 235 Radiochromic Film Dosimetry: An Update to TG-55. *Med Phys*. 2020;47(12):5986-6025. doi:10.1002/mp.14497

17. Looe HK, Büsing I, Tekin T, et al. The polarity effect of compact ionization chambers used for small field dosimetry. *Med Phys*. 2018;45(12):5608-5621. doi:10.1002/mp.13227

18. Partanen M, Niemelä J, Ojala J, Keyriläinen J, Kapanen M. Properties of IBA Razor Nano Chamber in small-field radiation therapy using 6 MV FF, 6 MV FFF, and 10 MV FFF photon beams. *Acta Oncol*. 2021;60(11):1419-1424. doi:10.1080/0284186X.2021.1979644

19. Lopez-Sánchez M, Pérez-Fernández M, Pardo E, et al. Small static radiosurgery field dosimetry with small volume ionization chambers. *Phys Med*. 2022;97:66-72. doi:10.1016/j.ejmp.2022.04.002

20. Hermida-López M, Sánchez-Artuñedo D, Rodríguez M, Brualla L. Monte Carlo simulation of conical collimators for stereotactic radiosurgery with a 6 MV flattening-filter-free photon beam. *Med Phys*. 2021;48(6):3160-3171. doi:10.1002/mp.14837

21. Shields L, Nikandrovs M, Vintró LL, Clean BM. Energy-dependence investigation for a range of clinically used detectors from 70 kV to 6 MV. *Med Phys*. 2023;50(1):582-589. doi:10.1002/mp.15857

22. Francescon P, Kilby W, Noll JM, Masi L, Satariano N, Russo S. Monte Carlo simulated corrections for beam commissioning measurements with circular and MLC shaped fields on the CyberKnife M6 System: a study including diode, microchamber, point scintillator, and synthetic microdiamond detectors. *Phys Med Biol*. 2017;62(3):1076-1095. doi:10.1088/1361-6560/aa5610

23. Underwood TSA, Winter HC, Hill MA, Fenwick JD. Detector density and small field dosimetry: integral versus point dose measurement schemes. *Med Phys*. 2013;40(8):082102. doi:10.1118/1.4812687